

## Nonlinear Dynamics of Collapse Phenomena in Heliotron Plasma with Large Pressure Gradient

N. Mizuguchi 1)2), Y. Suzuki 1), N. Ohyaabu 1)2)

1) National Institute for Fusion Science, Toki, Japan

2) The Graduate University for Advanced Studies (Sokendai), Toki, Japan

e-mail contact of main author: mizu@nifs.ac.jp

**Abstract.** We have executed nonlinear magnetohydrodynamic(MHD) simulations in a heliotron-type configuration with a large pressure gradient to reveal the nonlinear dynamics of collapse phenomena. The simulation results reproduce the qualitative characteristics of the experimental observation on the so-called core density collapse (CDC) events in the Large Helical Device (LHD) plasma with the super dense core (SDC) profile. A long-term nonlinear behavior on the event, including the flushing mechanism of the core pressure, is clarified. The simulation result shows the linear growth of the ballooning-like resistive instability modes with the intermediate poloidal wavenumbers. The growth of the modes are saturated soon, and the system experiences the energy relaxation in about 1 msec. It should be noted that the linear mode structures are localized in the edge region, whereas the core pressure rapidly falls as the system reaches the relaxed state. The co-existence of the edge perturbation and the core collapse is consistent with the experimental observations. The lost pressure forms a wider tail in the peripheral region. The core pressure is remarkably reduced at a certain period, while it had withstood the disturbance before it. The most salient feature on this period is the disordering of the magnetic field structure. The system keeps the nested-flux-surface structure well in the beginnings, whereas part of them are abruptly lost at this period. Such a situation can induce a flattening of the pressure profile along the reconnected field lines. By checking the place where the plasma loss due to this mechanism occurs, such plasma outlets are found to be located mainly on the disordered region. Thus, one can conclude that the core collapse can be caused by the disturbance of the magnetic field.

### 1. Introduction

In the recent larger toroidal experiments on an almost steady operation, events accompanied by an abrupt degradation of the confinement are often observed. Such collapse phenomena usually proceed in the magneto-hydrodynamic (MHD) time scale, sometimes accompanied by precursory oscillations, and are in general harmful to the confinement. To control the collapse phenomena is one of the key issues for the development of fusion sciences, and needs a proper understanding of their physical mechanism. Since the collapse phenomena are governed by highly nonlinear processes, it is helpful to make use of the numerical simulation technique.

In the recent helical experiments at high performance like the super-dense core (SDC) state of the Large Helical Device (LHD)[1], an abrupt flushing of the core density is occasionally observed. This event is named the core density collapse (CDC)[2]. CDCs are typically observed in the re-heating stage where the plasma beta gradually increases after the pellet injection. The crash phase of the CDCs are characterized by a rapid fall of the central density and its expulsion. CDCs are sometimes accompanied by the precursors in the outer region[3].

This article aims at providing the qualitative understanding of the nonlinear dynamics of a collapse phenomenon in the heliotron plasma with a large pressure gradient, which features the SDC state of the LHD, by means of a nonlinear MHD simulation. To seek the physical mechanisms of the realistic CDC event needs accurate stability analyses by comparing with the experiments, together with simulations with realistic parameters, which are actually unachievable with the present schemes, and is beyond our scope.

## 2. Simulation Model

To study the nonlinear behavior of the MHD fluid in a helical system, we solve the time development of the standard set of compressive, resistive, nonlinear MHD equations,

$$\frac{\partial \rho}{\partial t} = -\nabla \cdot (\rho \mathbf{v}), \quad (1)$$

$$\frac{\partial (\rho \mathbf{v})}{\partial t} = -\nabla \cdot (\rho \mathbf{v} \mathbf{v}) - \nabla p + \mathbf{j} \times \mathbf{B} + \mu \left( \nabla^2 \mathbf{v} + \frac{1}{3} \nabla (\nabla \cdot \mathbf{v}) \right), \quad (2)$$

$$\frac{\partial \mathbf{B}}{\partial t} = -\nabla \times \mathbf{E}, \quad (3)$$

$$\frac{\partial p}{\partial t} = -\nabla \cdot (p \mathbf{v}) - (\gamma - 1) (p \nabla \cdot \mathbf{v} + \eta j^2), \quad (4)$$

in a full-toroidal three-dimensional geometry. The variables,  $\rho$ ,  $\mathbf{v}$ ,  $\mathbf{B}$ , and  $p$  represent the mass density, the fluid velocity, the magnetic field, and the pressure, respectively. The current density  $\mathbf{j}$  and the electric field  $\mathbf{E}$  are calculated from

$$\mathbf{j} = \nabla \times \mathbf{B}, \quad (5)$$

$$\mathbf{E} = -\mathbf{v} \times \mathbf{B} + \eta \mathbf{j}. \quad (6)$$

In (1)-(6), the dissipation terms are included as the resistivity  $\eta$  and the viscosity  $\mu$ . These terms are assumed to be uniform constants for simplicity. The Ohmic heating term is evaluated in the evolution of the pressure  $p$ , whereas the viscous heating is ignored for simplicity. All the spatial derivatives are expressed numerically using the fourth order central difference scheme, together with the time integration solved by the fourth order Runge-Kutta method, as used in the previous simulations for tokamak[4].

To follow the geometry of the helical devices with continuously wound magnetic coils, we adopt the helical-toroidal coordinate system used in the HINT code[5], with the helical period  $h$  is  $10/2$  to follow the LHD configuration. The numbers of the numerical grid are  $62 \times 146$  for the poloidal cross section, and 500 for the toroidal direction.

The initial condition for the simulation is given by the numerical solution of the HINT2 code[6], which models an average experimental configuration of LHD with SDC. The pressure and the rotational transform ( $\iota$ ) profiles and the configuration are shown in Fig. 1. The simulation geometry includes the region out of the separatrix. To treat such an external region continuously from the inside of the separatrix, we artificially add a small uniform value to the pressure initially.

The simulation starts by adding tiny random perturbations to the velocity components of the initial equilibrium. Then, the spontaneous time development of the MHD system is solved by vector-parallel calculation on a supercomputer. All the quantities used throughout this article are treated as normalized ones with  $\rho_0=1$ ,  $R_0=1$ [m],  $B_0=1$ . Therefore, the unit of time are

expressed in the Alfvén transit time ( $\tau_A$ ), which roughly corresponds to 1 [ $\mu\text{sec}$ ] for the LHD experimental parameter.

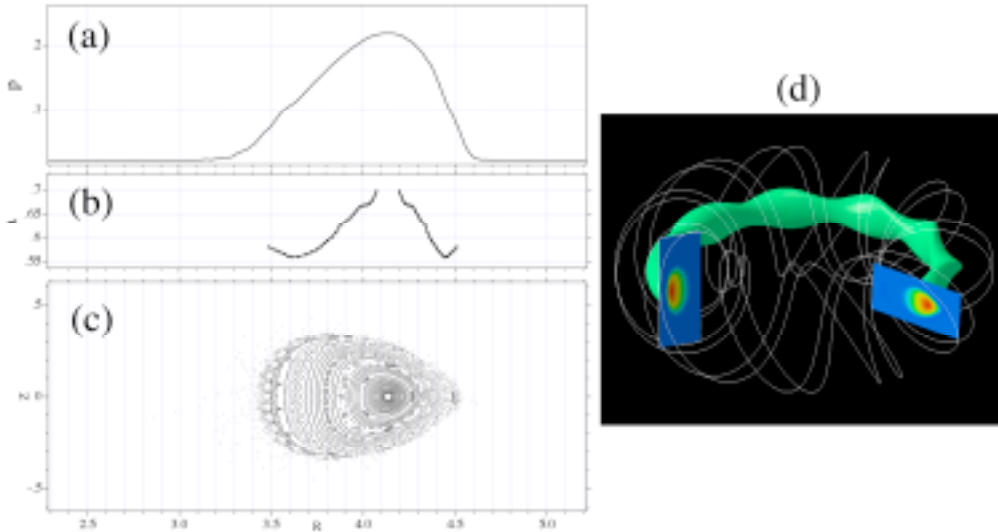


FIG. 1. The profiles of the initial equilibrium for (a) the radial pressure profile, (b) the radial rotational transform profile, (c) the puncture plot of the magnetic field for the horizontally elongated poloidal cross section, and (d) the three dimensional pressure profile.

### 3. Simulation Results

The perturbations applied on the initial equilibrium can develop exponentially with some eigenmode structures under unstable situations. For a large value of the resistivity the system tends to be unstable for the resistive instabilities. It should be noted that the simulation model used here cannot treat the pure ideal regime because the unavoidable numerical dissipations can act as the resistivity term depending on the grid size. To observe correctly the physical behavior of the MHD system without confusion due to such numerical resistivity, the simulation for the present grid size has to be executed with a large resistivity of  $\eta > 10^{-5}$ , which is much larger than the classical value for the conventional experiments. Although the non-realistic large resistivity may exaggerate the linear growth rate of the resistive instability modes, the simulation results would help us obtain the basic understanding of the nonlinear behaviors of the resistive modes. In the case for  $\eta = 10^{-4}$ , the instability begins to grow exponentially with some eigenmodes, where the total growth rate appears to be larger for the larger resistivity, indicating that the modes have the exact nature of the resistive ones. The results presented hereafter are of the case for  $\eta = 10^{-4}$ .

The structure of the eigenmode is shown in Fig. 2 with the contour of the perturbations in the pressure for the horizontally elongated poloidal cross section. One can see the mode component is poloidally localized in the outer region with the intermediate ( $m \sim 15$ ) components, where  $m$  is the poloidal mode number. Such a ballooning-like nature is seen in any toroidal direction. Moreover, the mode structure is almost identical for all of the horizontally elongated plane. This implies that the low- $n$  components are not so significant in this case.

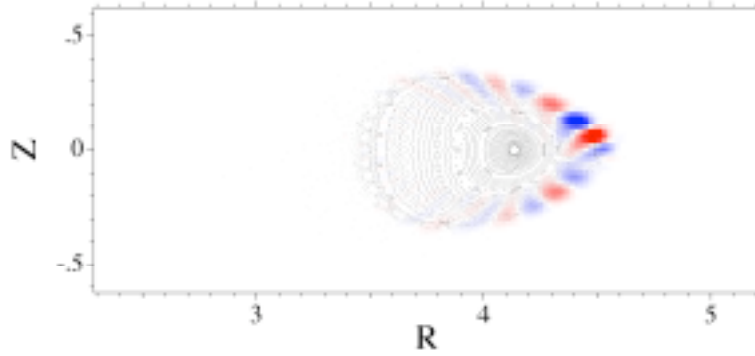


FIG. 2. The linear eigenmode structure. The perturbations in the pressure are plotted with color contours. The puncture plot of magnetic field for the initial condition is also shown.

As the amplitude of the perturbations becomes large, the configuration is deformed spontaneously into a visible scale, and the growth is saturated. The time development of the overall system is plotted with the change in the total kinetic energy in Fig 3(a). One can see the growth and the relaxation of the instability repeat three times in about  $500\tau_A$ . The corresponding change in the pressure profile is plotted in Fig 3(b) for the radial ones on the horizontally elongated equator. As shown in Fig. 3(b), or as expected, the edge pressure profile is disordered by the instability mode behaviors. Surprisingly, the central pressure is also drops as time goes on. This behavior is clearly shown in Fig 3(a) with the trace of the maximum pressure. The most rapid fall of the pressure is observed at around  $t=335\tau_A$ . The system reaches to the finally relaxed state just after the rapid pressure fall. In the final state, the pressure profile forms a wide tail in the peripheral region, as shown in Fig. 3(b).

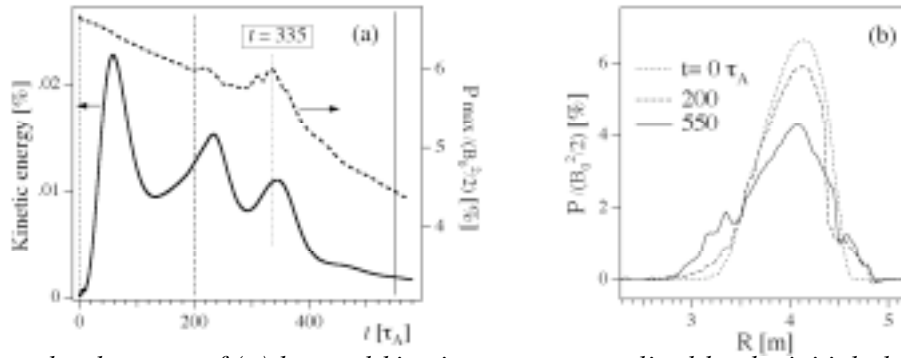


FIG. 3. Time development of (a) the total kinetic energy normalized by the initial plasma thermal energy and the maximum pressure, and (b) the pressure profile normalized by the initial magnetic energy on the magnetic axis.

The collapsing process is more clearly visualized by a two-dimensional contour plot of the pressure profile in a horizontally elongated poloidal cross section, as shown in Fig. 4. It can be seen that the structure is destroyed little by little from the peripheral region in the early stage ( $t \sim 130\tau_A$ ), reflecting the linear eigenmode behaviors. The convection motions of the eigenmodes form a number of the finger-like structures in the unstable region. Then, the disordered region is extended inward. However, the bulk of the plasma is not displaced away even when the rapid fall occurs ( $t > 335\tau_A$ ). This is a remarkable contrast to the previous simulation result for the spherical tokamak case[4], where the rapid fall of the core pressure is caused by a secondary induced internal low- $m/n$  instability.

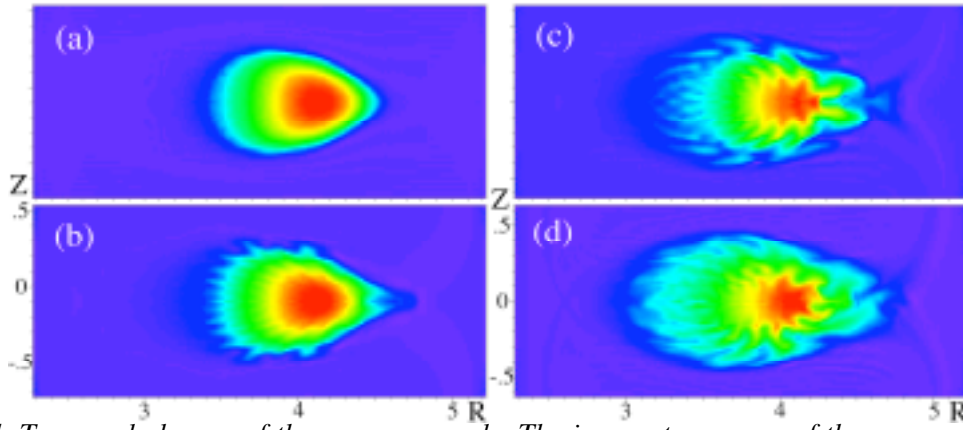


FIG. 4. Temporal change of the pressure profile. The iso-contour maps of the pressure on the horizontally elongated cross section are drawn at (a) $t=0$ , (b) $130$ , (c) $300$ , and (d) $550\tau_A$ .

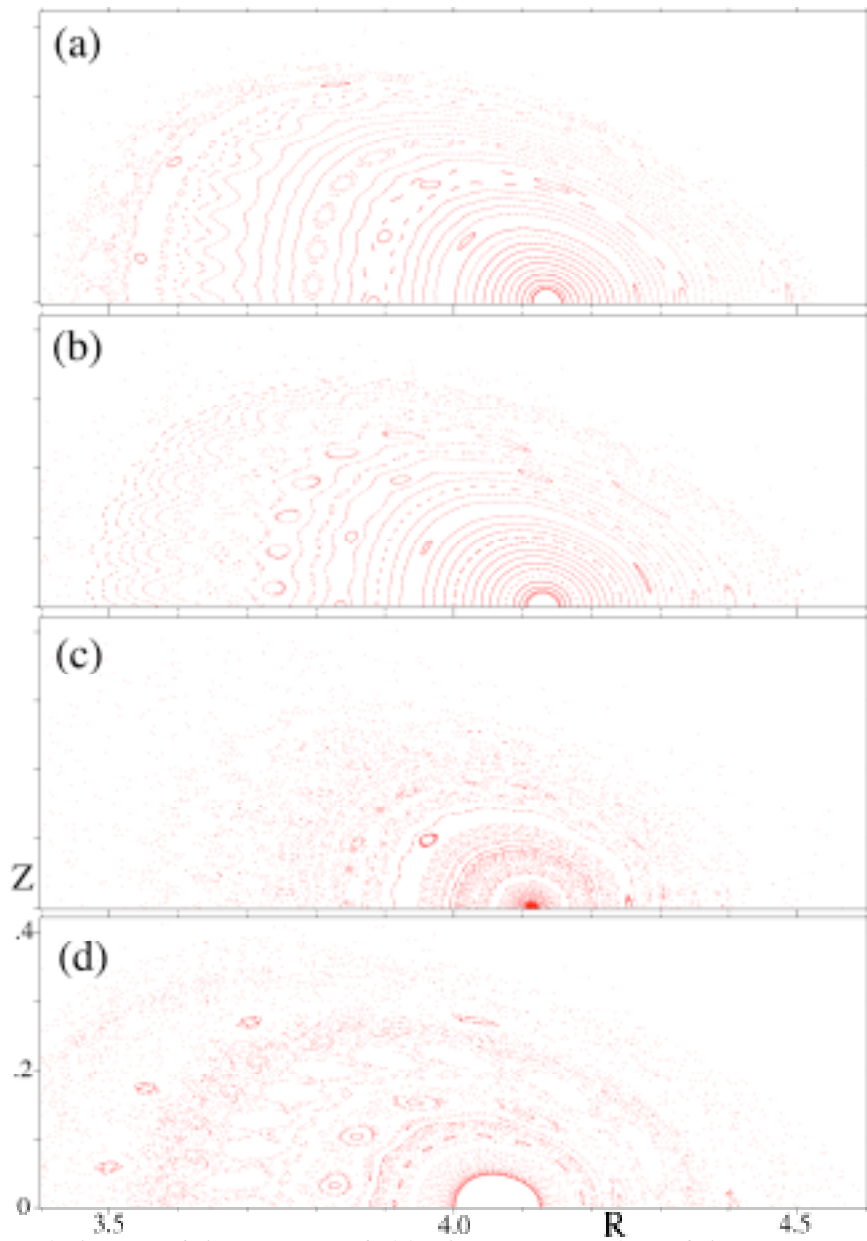


FIG. 5. Temporal change of the magnetic field. The puncture plots of the magnetic field lines on a horizontally elongated cross section are plotted at (a) $t=0$ , (b) $130$ , (c) $300$ , and (d) $550\tau_A$ .

The period of the core pressure fall at around  $t=335\tau_A$  is characterized by some qualitative transitions of the system. The most salient feature on this period is the disordering of the magnetic field structure. As shown in Fig. 5, the system keeps the structure of the nested flux surfaces well in the core region before  $t=335\tau_A$  [see Fig. 5(a)-(b)], whereas part of them are abruptly lost at around  $t=335\tau_A$  [Fig.5(c)]. As the core pressure fall ceases, the flux surfaces gradually reappear [Fig.5(d)]. Such a disordered magnetic structure can cause a flattening of the pressure profile in a wide range not only by the parallel transport process which is not taken into account in this model, but also by the parallel equilibration motion of MHD, as in this case. Therefore, one can consider the disordering of the magnetic structure the direct cause of the core pressure collapse.

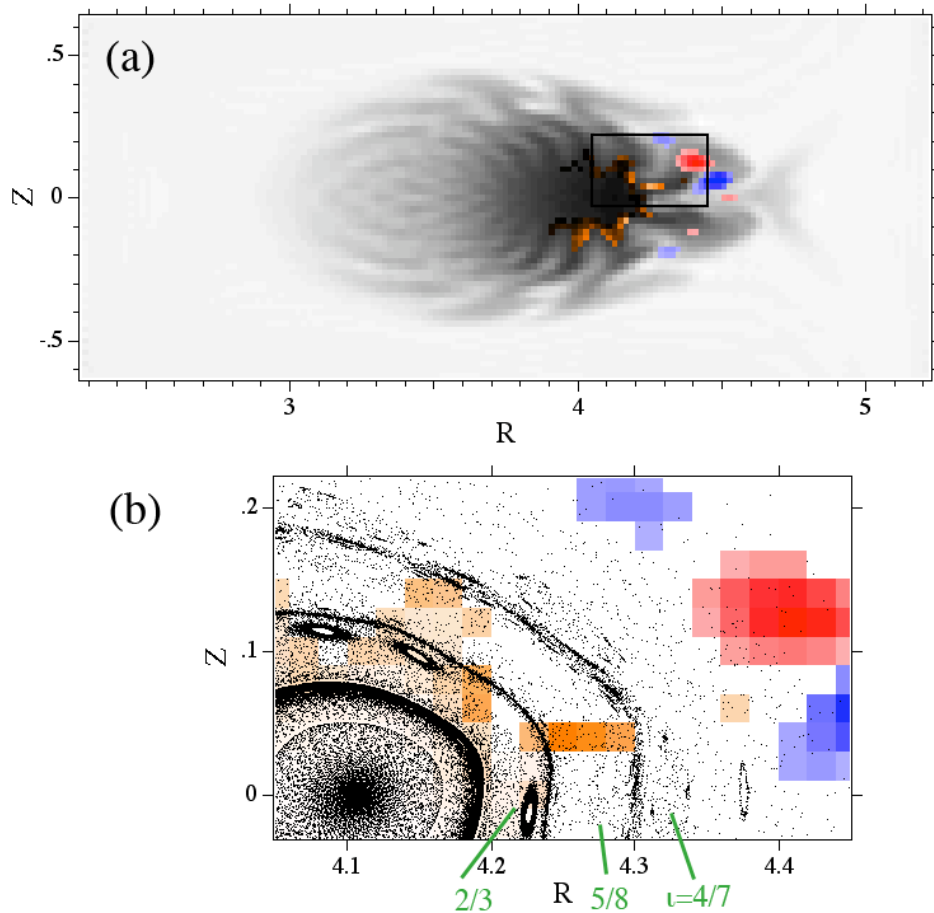


FIG. 6. The poloidal profiles of the plasma pressure energy flux at  $t=335\tau_A$ . (a) The contours of the absolute value of the energy flux  $|pV|$  (orange), the perturbations in the pressure in the linear eigenmode (red and blue), and the net pressure (gray). (b) The magnification of the box in (a) without the pressure but with the puncture plot of the magnetic field lines. The original locations of the rational surfaces for  $\nu=2/3$ ,  $5/8$ , and  $4/7$  are also specified.

This insight can be supported by another observation of the simulation result concerned with the plasma flow structures. To find the place where the plasma loss due to this mechanism occurs extensively, the amount of the internal energy flux  $|pV|$  is plotted with color contour in Fig.6(a) on the pressure profile indicated by the gray contour. One can see such plasma outlets are mainly located on the root of the fingers. Another simple analysis shows that the direction of the energy flux is almost parallel to the magnetic field. The neighboring magnetic structure is also shown in Fig. 6(b). The magnetic flux surfaces are hard to find except for the

regions between the islands or their ruins. In Fig. 6(b), one can see couple of clear surfaces at  $R=4.24$  m and  $4.30$  m on the equator ( $Z=0$ ), putting the ruins of the  $\iota=2/3$ ,  $5/8$ , and  $4/7$  islands between them, and that the outlets correspond to the disordered region. Thus, within the MHD framework, the magnetic and flow structures show that the core pressure can be expelled away through the disordered or reconnected field lines. It should also be noted that the spots of the outlets are seen apart from the original linear eigenmode ones which is shown with the red and blue contours in Fig.6.

#### **4. Discussion**

The simulation results described above can be compared in several points with the experimental observations. One of the most prominent collapse phenomena in the helical systems is the CDC in LHD. First, the time scale of the crash phase of the CDCs is of the order of sub-millisecond, which is comparable to the whole relaxation process of the simulation result. As mentioned above, the dissipation coefficients for the simulation are much larger than the realistic one, and the linear growth of the resistive modes may appear to be more rapid. However, since the nonlinear behaviors including the loss mechanism of the core pressure are dominated by the convection of the MHD fluid, the time scale would not be affected so much by the value of the resistivity. Secondly, the coexistence of the edge precursors and the core collapse in the experiment can be reasonably explained by the simulation result. The core collapse is not directly caused by the mode activities, but through the flattening of the pressure gradient due to the disordering of the magnetic structures. Under this scenario, the role of the precursor modes is only the trigger of the flushing of the core pressure. The magnitude and the time constant of the collapse would rather be governed by the global parameters such as the pressure gradient. Thirdly, the experimental observation that only the density drops, keeping the temperature profile unchanged, would show that the process is not governed by conductive process, but by convective one. The simulation result, which shows almost pure convective process, supports the observation.

This simulation result provides us with a basic understandings of the nonlinear behavior of the resistive modes. In the abovementioned result, the modes with intermediate wavenumbers are treated. However, the identification of the mode structures between the experiment and simulation is not yet pursued. The recent stability analysis for the LHD-SDC plasma[7] shows that the configuration is almost stable for the ideal modes. Therefore, if the operation is limited by instabilities, the control of the resistive modes would be important. More systematic analyses for the resistive modes are the next step of this study.

#### **5. Summary**

We have demonstrated the nonlinear dynamics of a heliotron plasma with a large pressure gradient on a collapse event induced by the ballooning-like resistive instability with an intermediate wavenumber. It has been clarified that the flushing of the core pressure is triggered by such the edge instabilities through the disordering of the magnetic field structures. The qualitative nature is comparative to the CDC event in the LHD. This model would provide us with the basic understanding of the MHD collapse events in the high- $\beta$  heliotron plasma.

**Acknowledgement**

The authors would like to thank Dr. Odachi, Dr. Sakamoto, Dr. Narushima and Dr. Miyazawa for their fruitful comments and discussion. This work is performed with the support and under the auspices of the NIFS Collaborative Research Program (NIFS08KNXN140) and a Grant-in-Aid for Scientific Research from the Japan Society for the Promotion of Science (No. 20760583).

**References**

- [1] Ohyaabu, N., et al., Phys. Rev. Lett. **97** (2006) 55002.
- [2] Sakamoto, R., et al., Plasma Fusion Res. **2** (2007) 047.
- [3] Odachi, S., et al., EX/8-2Rb, This conference.
- [4] Mizuguchi, N., et al., Nucl. Fusion **47** (2007) 579.
- [5] Harafuji, K., et al., J. Comp. Phys. **81** (1989) 169.
- [6] Suzuki, Y., et al., Nucl. Fusion **46** (2006) L19.
- [7] Narushima, Y., et al., J. Plasma Fusion Res., (in preparation).